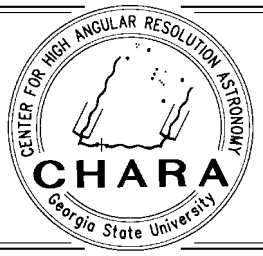

CHARA Technical Report

No. 96 February 2014

The CLASSIC/CLIMB Data Reduction: The Math

Theo ten Brummelaar

ABSTRACT: This technical report describes the methods used to extract closure phase from CLIMB data and visibility amplitude from both the CLASSIC and CLIMB beam combiners. It also includes a rather exhaustive description of the theory behind these methods. This high degree of detail is partly because previous publications of this theory contain errors, and partly because having done all this work it's nice to have it written up in full somewhere, and being slightly beyond the thesis writing stage, this is only possible for me in a technical report like this.

1. INTRODUCTION

At the time of writing this technical report, I know of five different data reduction codes for CLASSIC data, and at least two for CLIMB data. However, they all use pretty much the same methodology, and there is only one code set distributed to outside observers. In this document I will go over the theory of fringe production in a generalized N-way beam combiner and from there describe methods that can be used to extract visibility amplitudes and closure phases.

The derivation of the fringe theory will be done in some detail, and I apologize for that, but I have done this for two reasons. First, one rarely gets a chance to write these things out in full and a technical report such as this is one of the few places where this can be done. Second, there are inconsistencies in previous publications of this kind of analysis, including our original instrument paper (ten Brummelaar et. al. 2005)[2] and the paper on which that was based (Benson et. al. 1995)[3] The differences are minor, but worth clearing up.

The discussion of theory will be followed by a description of the software itself and how it might best be used. Should you feel you already understand the theory I suggest that you check that you understand Equations 22, 26, 27, 28 and 47 and then skip straight to the technical report on the data pipelines.

---

[1]Center for High Angular Resolution Astronomy, Georgia State University, Atlanta GA 30303-3083
Tel: (404) 651-2932, FAX: (404) 651-1389, Anonymous ftp: chara.gsu.edu, WWW: http://chara.gsu.edu

[2]In the CHARA Instrument paper I used ν for both frequency in the Fourier domain and for raw visibility amplitude. This is confusing, and should have been fixed before publication, but I only noticed this while doing the analysis described in this technical report.

[3]As discussed below, there is a factor of two difference between the Benson formulation and ours. No doubt most people get the software to work anyway. In our case I had made two different factor of 2 errors in the code, which compensated. This has been fixed.

2. THEORY

Here I will develop a general nomenclature and analysis of an arbitrary N-way beam combiner. We assume that N inputs beams are combined in some way and all beams are, to some extent at least, present in the output beam being considered. We do not require the same number of outputs as inputs as each output beam can be considered in isolation as an independent N-way combiner.

2.1. The Fringe Equation

Consider the output of an N-way beam combiner of any kind. We can write the electric field reaching the output of this beam combiner from each input beam i as

$$E_i(t) = A_i \cos(kx_i - kct + \phi_i) \tag{1}$$

where A_i is the amplitude of beam i, $k = \frac{2\pi}{\lambda}$, λ is the wavelength, x_i is the optical path length in input beam i, t is the time, c is the speed of light, and ϕ_i is the phase of the wavefront in input beam i. Note that this phase represents only the phase changes imposed within the beam combiner input.

The output of the beam combiner is then sensed using a camera of some kind which will measure the intensity, or time averaged modulus of the signal which we can write as

$$\begin{aligned}
S(k) &= \frac{1}{T}\int_0^T \left(\sum_{i=1}^{N} E_i(t)\right)^2 dt \\
&= \frac{1}{T}\int_0^T \left(\sum_{i=1}^{N} A_i \cos(kx_i - kct + \phi_i)\right)^2 dt \\
&= \sum_{i=1}^{N} A_i^2 \frac{1}{T}\int_0^T \cos^2(kx_i - kct + \phi_i)dt + \\
&\quad \sum_{i=1}^{N-1}\sum_{j=i+1}^{N} 2A_iA_j \frac{1}{T}\int_0^T \cos(kx_i - kct + \phi_i)\cos(kx_j - kct + \phi_j)\ dt
\end{aligned} \tag{2}$$

where ideally T is an integer multiple of $\frac{\lambda}{c}$, but it is sufficient that $T \gg \frac{\lambda}{c}$. Normally T is also much smaller than the fringe period.

We can simplify this considerably by firstly considering the second part of Equation 3 and expanding it as follows

$$\begin{aligned}
&\frac{1}{T}\int_0^T \cos(kx_i - kct + \phi_i)\cos(kx_j - kct + \phi_j)\ dt \\
= &\frac{1}{T}\int_0^T [\cos(kx_i + \phi_i)\cos(kct) + \sin(kx_i + \phi_i)\sin(kct)] \times \\
&[\cos(kx_j + \phi_j)\cos(kct) + \sin(kx_j + \phi_j)\sin(kct)]\ dt \\
= &\cos(kx_i + \phi_i)\cos(kx_j + \phi_j)\frac{1}{T}\int_0^T \cos^2(kct)\ dt + \\
&\cos(kx_i + \phi_i)\sin(kx_j + \phi_j)\frac{1}{T}\int_0^T \sin(kct)\cos(kct)\ dt +
\end{aligned}$$

$$\sin(kx_i + \phi_i)\cos(kx_j + \phi_j)\frac{1}{T}\int_0^T \cos(kct)\sin(kct)\ dt +$$
$$\cos(kx_i + \phi_i)\cos(kx_j + \phi_j)\frac{1}{T}\int_0^T \sin^2(kct)\ dt. \tag{3}$$

Now, given the standard integrals

$$\frac{1}{2\pi}\int_0^{2\pi} \cos^2 x\ dx = \frac{1}{2\pi}\int_0^{2\pi} \sin^2 x\ dx = \frac{1}{2} \tag{4}$$

and

$$\frac{1}{2\pi}\int_0^{2\pi} \cos x \sin x\ dx = 0. \tag{5}$$

we see that the cross terms in Equation 4 cancel to zero while the $\cos^2$ and $\sin^2$ integrals both are replaced by $\frac{1}{2}$ and we are left with

$$\begin{aligned} & \frac{1}{T}\int_0^T \cos(kx_i - kct + \phi_i)\cos(kx_j - kct + \phi_j)\ dt \\ = & \frac{1}{2}\left[\cos(kx_i + \phi_i)\cos(kx_j + \phi_j) + \sin(kx_i + \phi_i)\sin(kx_j + \phi_j)\right] \\ = & \frac{1}{2}\ \cos\left[k(x_i - x_j) + (\phi_i - \phi_j)\right]. \end{aligned} \tag{6}$$

We can now write the detected signal as

$$S(k) = \frac{1}{2}\sum_{i=1}^{N} A_i^2 + \sum_{i=1}^{N-1}\sum_{j=i+1}^{N} A_i A_j \cos\left[k(x_i - x_j) + (\phi_i - \phi_j)\right]. \tag{7}$$

If we use the signal intensity $I_i = A_i^2$ this becomes

$$S(k) = \frac{1}{2}\sum_{i=1}^{N} I_i + \sum_{i=1}^{N-1}\sum_{j=i+1}^{N} \sqrt{I_i I_j} \cos\left[k(x_i - x_j) + (\phi_i - \phi_j)\right]. \tag{8}$$

Since visibility amplitudes are normalized, that is they have a value between zero and one, the next step is to divide this signal by the mean intensity $\frac{1}{2}\sum_{i=1}^{N} I_i$ resulting in

$$N(k) = 1 + \sum_{i=1}^{N-1}\sum_{j=i+1}^{N} T_{ij} \cos\left[k(x_i - x_j) + (\phi_i - \phi_j)\right] \tag{9}$$

where we have introduced the transfer function

$$T_{ij} = \frac{2\sqrt{I_i I_j}}{\sum_{i=1}^{N} I_i}. \tag{10}$$

The Cittert-Zernike theory (See Born and Wolf for a derivation, or the original papers van Cittert (1934) and Zernike (1938)) tells us that the amplitude and phase of each fringe function from each baseline has an amplitude V_{ij} and a phase Φ_{ij} which are directly related

to the Fourier Transform of the intensity pattern on the sky and it is these things that we are ultimately interested in measuring. We therefore explicitly include these terms in the fringe equation and write

$$N(k) = 1 + \sum_{i=1}^{N-1} \sum_{j=i+1}^{N} T_{ij} V_{ij} \cos\left[k(x_i - x_j) + (\phi_i - \phi_j) + \Phi ij\right]. \tag{11}$$

As we shall see later, we will ultimately want to calculate a closure phase around a triangle of baselines, rather than the phase of a single baseline as the later is washed out by atmospheric noise.

Equation 11 is the fringe equation for an N-way beam combiner for a single wavelength. We now need to apply this equation to our actual beam combiners by introducing a finite bandwidth and the temporal fringe encoding used in CLIMB and CLASSIC.

First, we will assume that the delay lines have removed all optical path length differences (OPD) between the N beams and that the only OPDs are introduced by the so called 'dither mirrors' that each move at a constant velocity v_i and may be different for each beam. So we say that

$$x_i - x_j = (v_i - v_j)\ t = v_{ij}\ t. \tag{12}$$

It is also convenient to use the wave number

$$\sigma = \frac{1}{\lambda} = \frac{k}{2\pi}. \tag{13}$$

When we substitute Equations 12 and 13 into the fringe Equation 11 we get

$$N(\sigma) = 1 + \sum_{i=1}^{N-1} \sum_{j=i+1}^{N} T_{ij} V_{ij} \cos\left[2\pi\sigma v_{ij} t + (\phi_i - \phi_j) + \Phi ij\right]. \tag{14}$$

The final step is to introduce a finite bandwidth and integrate the fringe equation across this bandwidth. Let us for the sake of simplicity assume that the bandwidth is square, centered on σ_0 and with a width of $\Delta\sigma$. We then have

$$\begin{aligned} N(\sigma_0, \Delta\sigma) &= \frac{1}{\Delta\sigma} \int_{\sigma_0 - \frac{\Delta\sigma}{2}}^{\sigma_0 + \frac{\Delta\sigma}{2}} N(\sigma) d\sigma \\ &= \frac{1}{\Delta\sigma} \int_{\sigma_0 - \frac{\Delta\sigma}{2}}^{\sigma_0 + \frac{\Delta\sigma}{2}} \left(1 + \sum_{i=1}^{N-1} \sum_{j=i+1}^{N} T_{ij} V_{ij} \cos\left[2\pi\sigma v_{ij} t + (\phi_i - \phi_j) + \Phi ij\right]\right) d\sigma \\ &= 1 + \frac{1}{\Delta\sigma} \sum_{i=1}^{N-1} \sum_{j=i+1}^{N} T_{ij} V_{ij} \int_{\sigma_0 - \frac{\Delta\sigma}{2}}^{\sigma_0 + \frac{\Delta\sigma}{2}} \cos\left[2\pi\sigma v_{ij} t + (\phi_i - \phi_j) + \Phi ij\right] d\sigma. \end{aligned} \tag{15}$$

Note that we have assumed that the visibility V_{ij} and transfer function T_{ij} are constant within the small bandwidth of our optical filter.

Let's consider the integral part of Equation 16 which becomes easier if we make the substitution $\eta = \sigma - \sigma_0$ and we get

$$I = \int_{\sigma_0 - \frac{\Delta\sigma}{2}}^{\sigma_0 + \frac{\Delta\sigma}{2}} \cos\left[2\pi\sigma v_{ij} t + (\phi_i - \phi_j) + \Phi ij\right] d\sigma$$

$$
\begin{aligned}
&= \int_{-\frac{\Delta\sigma}{2}}^{+\frac{\Delta\sigma}{2}} \cos\left[2\pi(\sigma_0+\eta)v_{ij}t + (\phi_i-\phi_j) + \Phi ij\right] d\eta \\
&= \frac{1}{2\pi v_{ij}t}\left[\sin\left(2\pi(\sigma_0+\eta)v_{ij}t + (\phi_i-\phi_j) + \Phi ij\right)\right]_{-\frac{\Delta\sigma}{2}}^{+\frac{\Delta\sigma}{2}} \\
&= \frac{1}{2\pi v_{ij}t}\left[\sin\left(\pi\Delta\sigma v_{ij}t + C\right) - \sin\left(-\pi\Delta\sigma v_{ij}t + C\right)\right] \qquad (16)
\end{aligned}
$$

where

$$C = 2\pi\sigma_0 v_{ij}t + (\phi_i - \phi_j) + \Phi ij. \qquad (17)$$

Now, it also simple to show that

$$
\begin{aligned}
\sin(a+b) - \sin(a-b) &= \sin(a)\cos(b) + \sin(b)\cos(a) - \sin(a)\cos(b) + \sin(b)\cos(a) \\
&= 2\sin(b)\cos(a) \qquad (18)
\end{aligned}
$$

and in our case $a = C$ and $b = \pi\Delta\sigma v_{ij}t$, so combining Equations 16, 17, 17 and 19 we arrive at the final fringe equation for an N-way beam combiner with a finite square bandpass

$$N(\sigma_0, \Delta\sigma) = 1 + \sum_{i=1}^{N-1}\sum_{j=i+1}^{N} T_{ij}V_{ij}\ \mathrm{sinc}\left[\pi\Delta\sigma v_{ij}t\right]\cos\left[2\pi\sigma_0 v_{ij}t + (\phi_i-\phi_j) + \Phi ij\right]. \qquad (19)$$

This is the result we're all used to seeing: oscillating terms for the fringes from each baseline, whose fringe period is a function of the central wavelength of the optical filter, modulated by an envelope function, in this case a sinc function, whose size is inversely proportional to the width of the optical filter. In this analysis we have assumed that the optical filter is square, or a 'top hat' function, whose Fourier Transform is a sinc function, and as we shall see, this works in general. That is, the fringe envelope function is the Fourier transform of the filter function. This is the basis for Fourier Transform Spectroscopy, but that is beyond the realm of this technical report.

Everything that now follows is now based on Equation 19, the generalized fringe equation for an N-way beam combiner.

2.2. Application of the Fringe Equation to CLASSIC

CLASSIC is a simple open air aperture plane beam combiner[4] consisting of one beam combiner and one dispersion compensation plate, hence the name. The optical layout of CLASSIC is given in Figure 1. For simplicity, let's assume that the visibility phase $\Phi_{12} = 0.0$. Since the atmospherically induce piston noise will overwhelm that phase anyway this is probably the only assumption one can usefully make. We will also assume that the delay lines are adjusted such that there is no phase difference between the beams at the point they are combined on the beam splitter and for the time being we will ignore atmospheric and detector noise.

[4]Note that I am avoiding the term "Michelson beam combiner", a terminology that is misleading - Michelson's stellar interferometer created fringes in the image plane, not the aperture plane, and was in fact a "Fizeau beam combiner", another misleading term.

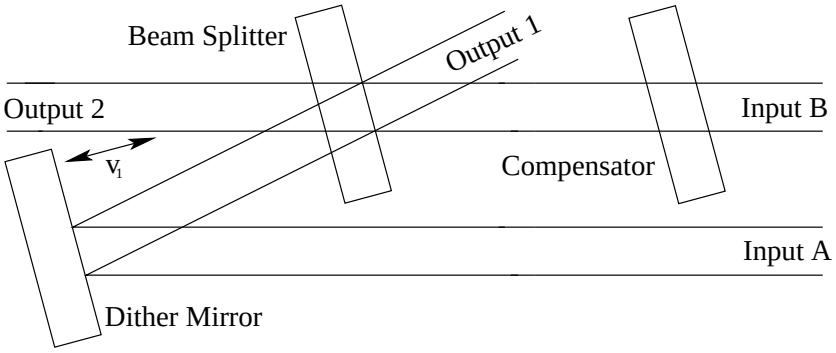

FIGURE 1. Schematic of the optical layout of the CLASSIC beam combiner.

In this simple case of a two beam combiner the transfer function in Equation 10 reduces to

$$T_{AB} = \frac{2\sqrt{I_A I_B}}{I_A + I_B}. \tag{20}$$

which is exactly the same as the transfer function given in Benson et al. (1995) and all the other papers that cite it except that we now use A and B for the two input beams instead of 1 and 2. As we shall see below this helps to remove some confusion between input and output beams. If the two beams have equal intensity, that is $I_A = I_B$, we find that $T_{AB} = 1$ as one would expect.

Next, we need to establish the values of ϕ_1 and ϕ_2. First, note that these phase shifts will have different values for each of the output beams. We will, therefore, now use the notation ϕ_{ki} to represent the phase of input beam i in output k. Now, if we consider output 1 first, input beam A is transmitted through the beam splitter and so will undergo no phase change, so $\phi_{1A} = 0$, while input beam B is reflected and will therefore undergo a π phase change so $\phi_{1B} = \pi$. Similar reasoning gives us $\phi_{2A} = \pi$ and $\phi_{2B} = 0$. This results in a 2π phase difference between the two outputs, giving a bright or dark fringe on both sides of the beam splitter at the same time, and this is a violation of the conservation of energy. This bothered me for some time, and I even went so far as to go through this line of reasoning with several colleges who where all as confused as I was.

It turns out it is a common mistake (for students!), as discussed by Zetie et al (2000) - the reflection of input A inside the beam splitter is on a glass-air interface, that is a high refractive index to a low refractive index interface, and this beam does not undergo the π phase change we normally associate with reflections on mirrors, which have a low to high refractive index interface. With this cleared up we can see that

$$\phi_{1A} = 0,\ \phi_{1B} = \pi,\ \phi_{2A} = 0,\ \text{and}\ \phi_{2B} = 0. \tag{21}$$

We now have a π phase difference between the two outputs giving us the bright fringe on one side and a dark fringe on the other, as we know it should be, for only then is energy conserved.

We can therefore write the fringe equation for output i of CLASSIC as

$$N_i(\sigma_0, \Delta\sigma) = 1 + (-1)^i\ T_{iAB}\ V_{AB}\ \mathrm{sinc}\left[\pi\Delta\sigma vt\right] \cos\left[2\pi\sigma_0 vt + \Phi_{AB}\right]. \tag{22}$$

where we include an extra subscript for the transfer function T_{iAB} to acknowledge the fact that, due to imperfections and misalignment in the optics, the two output pixels will not

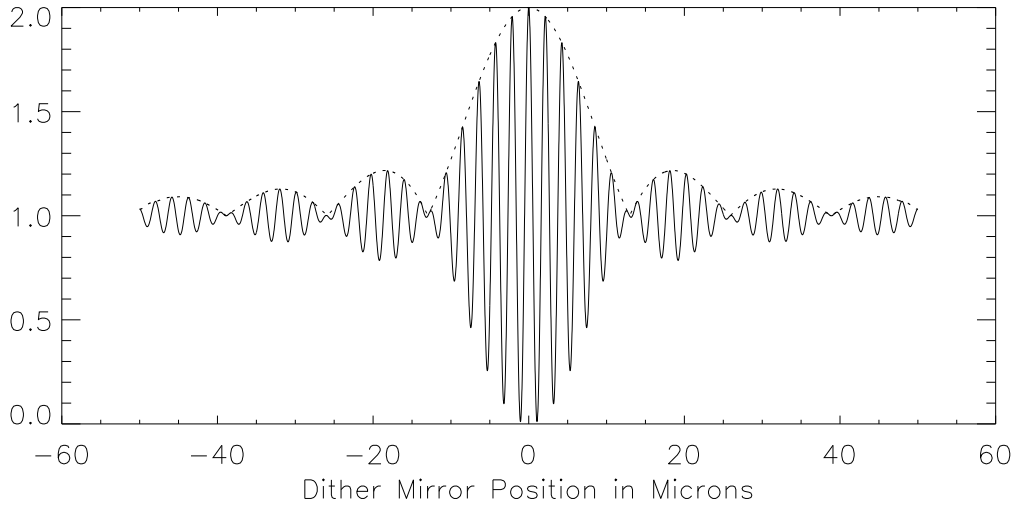

FIGURE 2. Example of a noiseless fringe signal for the CLASSIC beam combiner. The fringe envelope is shown with a dotted line. Note that the other output would have an identical envelope function but with the central fringe at 0 instead of 2.

necessarily have the same amount of light from each input beam and may therefore have different transfer functions.

As for Equation 20, this fringe equation for CLASSIC, Equation 22, is the same as that given in both Benson et al. (1995) and ten Brummelaar et al. (2005), although in the later there is an error in the notation for the visibility amplitude[5]. An example of a noiseless normalized fringe signal for output 1 for the K' band is given in Figure 2.

2.3. Application of the Fringe Equation to CLIMB

CLIMB is an extension of CLASSIC to three beams, thus the name CLassic Interferometry with Multiple Baselines. The optical layout of CLIMB is given in Figure 3. Here, one of the output beams of the CLASSIC layout is combined with a third beam. Note that his means, even in a perfect world, while each output will have the same total amount of light, they will not have the same amount of light from each input. As for CLASSIC, we need to include an extra subscript to the transfer function to indicate which output we are using, so for output i and input beams j and k we write

$$T_{ijk} = \frac{2\sqrt{I_{ij} I_{ik}}}{I_{iA} + I_{iB} + I_{iC}} \tag{23}$$

If we assume perfect optics, the transfer functions for the three output pixels for each beam pair, or baseline, are given in Table 1.

Now, in order to ensure that each baseline fringe pattern has a unique fringe frequency, the

[5]The aforesaid multiple use of the symbol ν

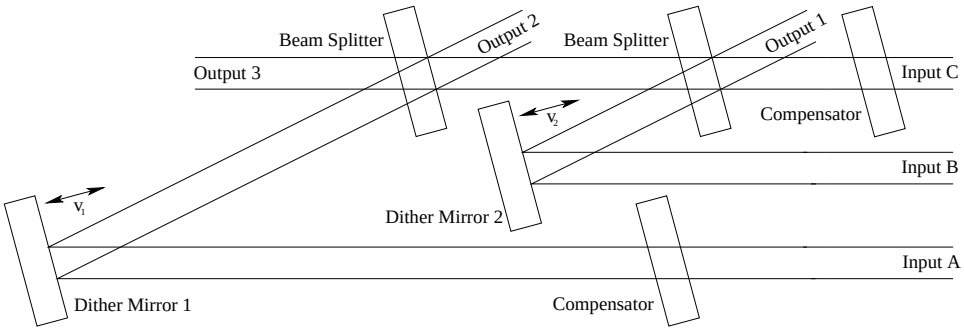

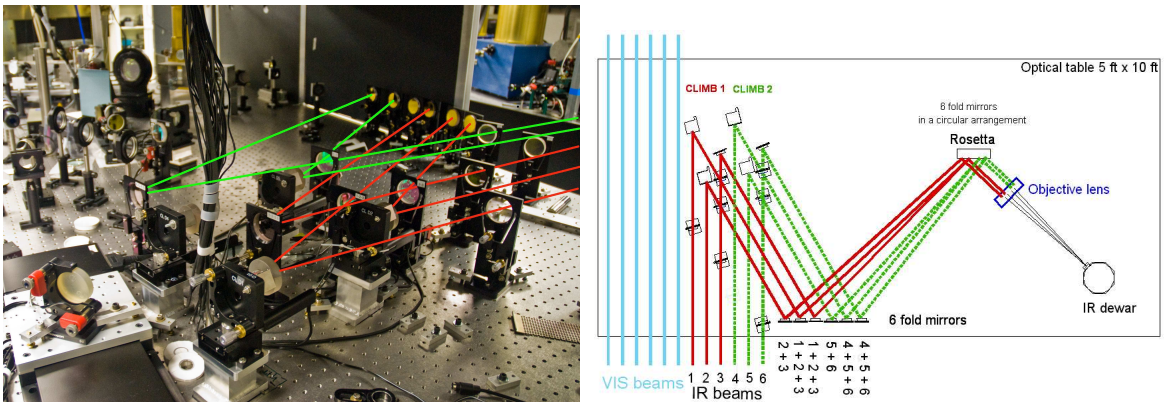

FIGURE 3. (Top) Schematic of the optical layout of the CLIMB beam combiner. (Bottom) Picture (Left) and schematic (right) of the CLIMB/CLASSIC optics with optical paths drawn. One CLIMB beam combiner is at the bottom (red beams) while a second CLIMB, in this instance configured for two beam CLASSIC operation, is at the top (green beams).

dither mirror velocities are set such that

$$v_1 = v, \quad \text{and} \quad v_2 = -2v \tag{24}$$

where v is the desired lowest fringe frequency. In order to keep things clear, we have not explicitly included the fact that the beam angle of reflection is 15 degrees and written these equations as if the reflection was 0 degrees. Furthermore, note that the mirrors move in opposite directions and that the range of motion of the second dither mirror is half that of the first. The result is that

$$v_{AB} = 3v, \quad v_{BC} = -2v, \quad \text{and} \quad v_{CA} = -v. \tag{25}$$

TABLE 1. CLIMB transfer functions for perfect optics.

Output	T_{AB}	T_{BC}	T_{CA}
1	0	1	0
2	$\frac{1}{\sqrt{2}}$	$\frac{1}{2}$	$\frac{1}{\sqrt{2}}$
3	$\frac{1}{\sqrt{2}}$	$\frac{1}{2}$	$\frac{1}{\sqrt{2}}$

The sign of v_{CA} is negative because when we come to measure closure phase we need to have a closed triangle and $v_{CA} = -v_{AC}$.

The last thing we need is the phase change for each beam on each output, which can be calculated in the same way as for CLASSIC. These phase changes are set out in Table 2.

TABLE 2. CLIMB phases for perfect optics. Note that beam A does not reach output 1 and so no phase is given.

Output	ϕ_A	ϕ_B	ϕ_C
1	-	0	π
2	0	π	π
3	0	0	0

We write the three outputs of the CLIMB beam combiner as

$$N_1(\sigma_0, \Delta\sigma) = 1 \quad - \quad T_{1BC}\ V_{BC}\ \mathrm{sinc}\left[2\pi\Delta\sigma vt\right] \cos\left[4\pi\sigma_0 vt - \Phi_{BC}\right] \tag{26}$$

$$\begin{aligned} N_2(\sigma_0, \Delta\sigma) = 1 \quad &- \quad T_{2AB}\ V_{AB}\ \mathrm{sinc}\left[3\pi\Delta\sigma vt\right] \cos\left[6\pi\sigma_0 vt + \Phi_{AB}\right] \\ &+ \quad T_{2BC}\ V_{BC}\ \mathrm{sinc}\left[2\pi\Delta\sigma vt\right] \cos\left[4\pi\sigma_0 vt - \Phi_{BC}\right] \\ &- \quad T_{2CA}\ V_{CA}\ \mathrm{sinc}\left[\pi\Delta\sigma vt\right] \cos\left[2\pi\sigma_0 vt - \Phi_{CA}\right] \end{aligned} \tag{27}$$

$$\begin{aligned} N_3(\sigma_0, \Delta\sigma) = 1 \quad &+ \quad T_{3AB}\ V_{AB}\ \mathrm{sinc}\left[3\pi\Delta\sigma vt\right] \cos\left[6\pi\sigma_0 vt + \Phi_{AB}\right] \\ &+ \quad T_{3BC}\ V_{BC}\ \mathrm{sinc}\left[2\pi\Delta\sigma vt\right] \cos\left[4\pi\sigma_0 vt - \Phi_{BC}\right] \\ &+ \quad T_{3CA}\ V_{CA}\ \mathrm{sinc}\left[\pi\Delta\sigma vt\right] \cos\left[2\pi\sigma_0 vt - \Phi_{CA}\right] \end{aligned} \tag{28}$$

Output 1 only receives light from inputs B and C and so has a fringe pattern exactly like that of Output 1 of CLASSIC, so it is not surprising that Equations 26 and 22 are very much alike. Outputs 2 and 3 receive light from all three input beams and so contain a fringe pattern from each baseline, each with a unique frequency. An example of a noise free signal with a visibility of 1 on all baselines and perfect optics from CLIMB output 3 is given in Figure 4. Note that the phase of inputs B and C Φ_{BC} is negative in each case because of the definition of the velocities above. Similarly, the phase Φ_{CA} is also negative because, as mentioned above, $\Phi_{AC} = -\Phi_{CA}$ and when it comes time to form a proper close phase we will be interested in Φ_{CA}.

Note that Equations 22, 26, 27, and 28 do not explicitly include phase noise due to the atmosphere. We need to also keep in mind that the visibility amplitude will vary due to atmospheric seeing.

2.4. Extracting Visibility Amplitude from the Data

The point of all of this is to measure the visibility amplitude and phase. We will deal with phase in sub-section 2.5, here we will only consider visibility amplitude. To keep things simple, and general, we will assume that the fringes from each baseline can be separated. In the case of CLASSIC this is of course trivial, in the case of CLIMB it requires bandpass

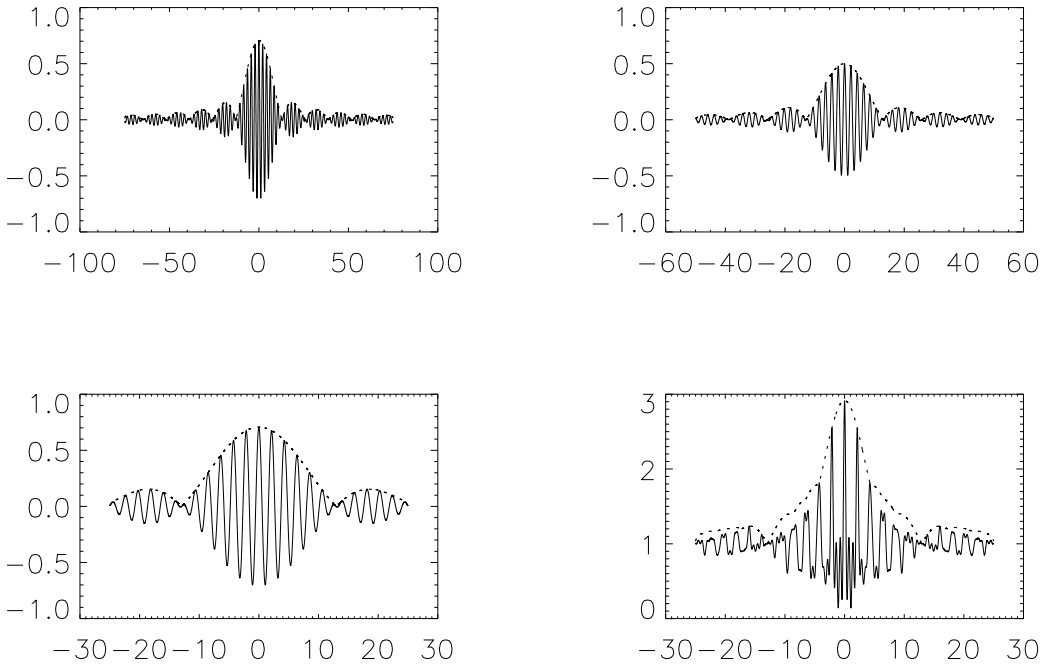

FIGURE 4. Example of noiseless fringe signals for the CLIMB beam combiner. The top three plots show the fringe signal from the A-B (top), B-C and C-A baselines plotted against the total amount of path introduced by the dither mirrors. The plot at the bottom shows the combination seen at output 3 against the position of Dither 1. The envelope is plotted as a dotted line in all four plots.

filters at the appropriate frequencies. So in the remainder of this analysis will we will use the simplified fringe equation

$$f(t) = V \ \mathrm{sinc}\left[\pi \Delta\sigma v t\right] \cos\left[2\pi\sigma_0 v t + \Phi\right]. \tag{29}$$

In real data there will be sources of noise, like atmospheric wavefront distortions, atmospheric piston, photon noise, and read-out noise from the camera, and so even in high signal to noise data the fringe pattern will be hard to detect and measure. A fit of Equation 29 to the data will not work very well in low signal to noise situations.

There have been two approaches used to get around this problem - one in the time domain and one in the frequency domain - and I will deal with these separately.

2.4.1. Time Domain Amplitude Estimation

In high signal to noise data it is possible to normalize and filter the signal and produce something that can be compared directly to Equation 29. If we divide the raw signal by a low pass filtered version of the scan we remove the scintillation noise, and at the same time normalize the data. We than pass this through a bandpass filter centered on the expected fringe frequency which leaves us with a relatively clean fringe signal. An example of this process is shown in Figure 5. We now have something that looks very much like Figure 2.

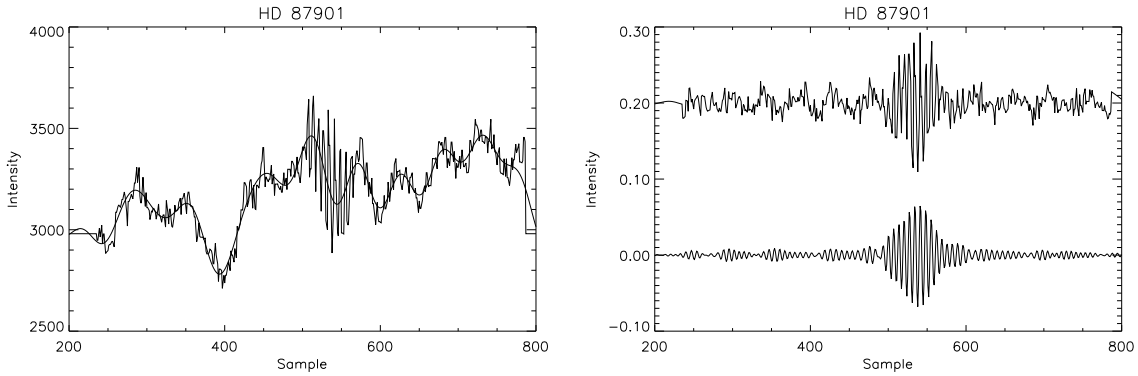

FIGURE 5. A fringe scan from CLASSIC is shown above in its raw signal form (top) with the low-pass filtered version superimposed prior to normalization. The bottom frame shows the same scan, with an offset of 0.2 for clarity, after normalization and, finally, after implementation of the band-pass filter.

There are, of course, numerous differences between the theoretical perfect signal and the real signal. Most notably, the lack of clear side lobes and the asymmetry of the fringe envelope. The former is simple a result of a lack of signal to noise - in very high signal to noise data the side lobes are quite clear. The later is primarily due to differential dispersion. The example data in Figure 5 where taken at a time when the Longitudinal Dispersion Correctors where not being used, and I will not cover in dispersion in any more detail in this technical report. If you're interested in dispersion affects see Dave Berger's thesis, or ten Brummelaar (1995).

The simplest way to extract a visibility amplitude estimate from the filtered fringe signal is to simple look for the maximum absolute amplitude. This is very fast, but has very little else to recommend it. For example, the digitized sampling of the data may not fall exactly on the fringe peak and so will almost always underestimate the fringe amplitude. Originally this was the way the real-time software estimate for visibility amplitude was calculated, but it is seldom used now. In the reduction pipeline this is referred to as the V_CMB visibility estimate.

A slightly better method is to find the peak of the fringe envelope, but first one needs to calculate that envelope. This can be done by demodulating the signal using a Hilbert Transform[6]:

1. Fourier transform the data.
2. Set the amplitude of all negative frequencies to zero.
3. Inverse transform the data.
4. Calculate the modulus of the result.

The final modulus is the fringe envelope, and this is the way the fringe envelopes in Figures 5 and 4 where calculated. The maximum amplitude of the envelope function is an estimate of

[6]This is the same way AM radio works

the fringe amplitude, and further more, it's position gives you a group delay measurement. Since you are filtering the data anyway, it is highly likely that you are already using Fourier transforms and so this method is still very fast, and it is much less susceptible to digitization errors. This is the estimator used by the real-time software, and also one of the many ways it can track the fringe position. In the reduction pipeline software this is referred to as the V_ENV visibility estimate.

If the signal to noise is high enough it is also possible to directly fit Equation 29 directly to the bandpass filtered and normalize data. This is more time consuming that either of the methods above, but gives estimates for parameters other than visibility amplitude. Furthermore, for separated fringe packet binaries Fringe fitting of this kind is essential in order to properly measure the fringe peak location and amplitude for each star (O'Brien et al. 2011). This method fails for lower signal to noise data, but has been used in a great many of our papers published to date. In the reduction pipeline software this is referred to as the V_FIT visibility estimate.

2.4.2. Frequency Domain Amplitude Estimation

If the signal to noise is too low, it is not possible to analyze the fringes in the time domain, but it is still sometimes possible to use the frequency domain. This is in fact the most common method of calculating visibility amplitude. One problem here is that a frequency domain, or spectral analysis, almost always involves the use of a Fourier transform and there are multiple normalizations for Fourier transforms. I believe it is the multiple ways of defining a Fourier transform that has resulted in most of the errors, or differences, in the published literature on this subject.

Since we use Numerical Recipes in C (Press et al., 1992) in the reduction code, we will use the normalization used by them. We write the Fourier transform of the function $h(t)$ as $H(f)$ and they are related via the relations

$$H(f) = \int_{-\infty}^{\infty} h(t) e^{2\pi i f t} dt \tag{30}$$

and

$$h(t) = \int_{-\infty}^{\infty} H(f) e^{-2\pi i f t} df. \tag{31}$$

We need to find the Fourier transform of Equation 29. Since it is a the multiple of two functions, the Fourier transform will be the convolution of the transforms of those two functions. So, we need the transform a sinc function and of a cos function. We could look these up, but the one needs to be very careful about the normalization used by the reference you use. In order to be certain, we can do the transforms ourselves. More specifically, since we have a good idea of what the answer is we can do an inverse transform which in this case is much easier.

So, consider the function $\delta(f-a)+\delta(f+a)$. The inverse transform of this function will be

$$\begin{aligned} & \int_{-\infty}^{\infty} \delta(f-a) e^{-2\pi i f t} df + \int_{-\infty}^{\infty} \delta(f+a) e^{-2\pi i f t} df \\ = \;& e^{2\pi i t a} + e^{-2\pi i t a} \\ = \;& \cos(2\pi t a) + i \sin(2\pi t a) + \cos(-2\pi t a) + i \sin(-2\pi t a) \\ = \;& 2\cos(2\pi t a) \end{aligned} \tag{32}$$

and so we have the Fourier transform pair

$$\cos(2\pi ta) \rightleftharpoons \frac{1}{2}(\delta(f-a)+\delta(f+a)). \tag{33}$$

In the case of our fringe Equation 29 $a = \sigma_0 v$ and so

$$\cos\left[2\pi\sigma_0 vt\right] \rightleftharpoons \frac{1}{2}(\delta(f-\sigma_0 v)+\delta(f+\sigma_0 v)) \tag{34}$$

where we have ignored the phase Φ. This is safe to do because of the standard Fourier relationship

$$f(t-a) \rightleftharpoons e^{-2\pi iaf}F(f). \tag{35}$$

When we take the power spectrum of this, that is the squared modulus, the exponential term will collapse to 1. Another way of looking at this is to say that phase does not affect the total power in a signal, and as we shall see, it is the total power that is of interest here.

We next consider the function $\frac{1}{a}\Pi\left(\frac{f}{a}\right)$, where

$$\Pi(x) = \begin{cases} 0, & |x| > \frac{1}{2} \\ \frac{1}{2}, & |x| = \frac{1}{2} \\ 1, & |x| < \frac{1}{2} \end{cases} \tag{36}$$

whose inverse Fourier transform will be

$$\begin{aligned} & \int_{-\infty}^{\infty} \frac{1}{a}\Pi\left(\frac{f}{a}\right) e^{-2\pi ift} df \\ = & \frac{1}{a}\int_{-\infty}^{\infty} \Pi\left(\frac{f}{a}\right)(\cos(2\pi ft)+i\sin(2\pi ft))\, df \\ = & \frac{1}{a}\int_{\frac{-a}{2}}^{\frac{a}{2}} (\cos(2\pi ft)+i\sin(2\pi ft))\, df \\ = & \frac{1}{2\pi ta}\left[\sin(2\pi ft)+i\cos(2\pi ft)\right]_{\frac{-a}{2}}^{\frac{a}{2}} \\ = & \frac{1}{2\pi ta}\left[\sin(\pi ta)-\sin(-\pi ta)+i(\cos(\pi ta)-\cos(-\pi ta))\right] \\ = & \frac{\sin(\pi ta)}{\pi ta} = \mathrm{sinc}(\pi ta). \end{aligned} \tag{37}$$

So we now have the Fourier pair

$$\mathrm{sinc}(\pi ta) \rightleftharpoons \frac{1}{a}\Pi\left(\frac{f}{a}\right) \tag{38}$$

where this time Equation 29 gives us $a = \Delta\sigma v$ so we get

$$\mathrm{sinc}(\pi t\Delta\sigma v) \rightleftharpoons \frac{1}{\Delta\sigma v}\Pi\left(\frac{f}{\Delta\sigma v}\right). \tag{39}$$

This demonstrates that the envelope function, in this case a sinc, and the optical filter function, in this case a top hat function, form a Fourier pair.

The next step is to use the standard Fourier relation

$$f(t)g(t) \rightleftharpoons F(f) * G(f). \tag{40}$$

So combining Equations 29, 34, 39, and 40 results in the Fourier Transform of the simple fringe equation

$$\begin{aligned} F(f) &= \frac{V}{\Delta\sigma v}\Pi\left(\frac{f}{\Delta\sigma v}\right) * \frac{1}{2}(\delta(f-\sigma_0 v) + \delta(f+\sigma_0 v)) \\ &= \frac{V}{2\Delta\sigma v}\left[\Pi\left(\frac{f-\sigma_0 v}{\Delta\sigma v}\right) + \Pi\left(\frac{f+\sigma_0 v}{\Delta\sigma v}\right)\right] \end{aligned} \tag{41}$$

and the power spectrum will therefore be

$$\mathrm{PS}(f(t)) = \frac{V^2}{4\Delta\sigma^2 v^2}\left[\Pi\left(\frac{f-\sigma_0 v}{\Delta\sigma v}\right) + \Pi\left(\frac{f+\sigma_0 v}{\Delta\sigma v}\right)\right]^2. \tag{42}$$

The last step is to integrate this power spectrum, which since it is symmetric, we will only do over the positive frequencies

$$\begin{aligned} S &= \int_0^\infty \mathrm{PS}(f(t))df \\ &= \frac{V^2}{4\Delta\sigma^2 v^2}\int_0^\infty \Pi^2\left(\frac{f-\sigma_0 v}{\Delta\sigma v}\right)df. \end{aligned} \tag{43}$$

Now, we know that

$$\int_{-\infty}^{\infty}\Pi^2(x)dx = \int_{\frac{-1}{2}}^{\frac{1}{2}}\Pi^2(x)dx = 1 \tag{44}$$

and so, using the substitution $x = \frac{f-\sigma_0 v}{\Delta\sigma v}$ we find that $dx = \frac{df}{\Delta\sigma v}$ and the result is that

$$\int_0^\infty \Pi^2\left(\frac{f-\sigma_0 v}{\Delta\sigma v}\right)df = \Delta\sigma v. \tag{45}$$

So, the total power S in the fringe power spectrum will be

$$S = \frac{V^2}{4\Delta\sigma v}, \tag{46}$$

which gives us our estimator for V^2

$$V^2 = 4\Delta\sigma v S. \tag{47}$$

This is the same as the result in Benson et al. (1995) except for a factor of 2. This factor of 2 is a result of doing the integration over positive frequencies only, rather than all frequency space.

All of this assumes that there is no noise in the data, which is of course not true. However, since we can assume that any noise is not correlated with the fringe signal, the power spectra of the signal and of the noise add and, if we can measure the noise power spectra, it can

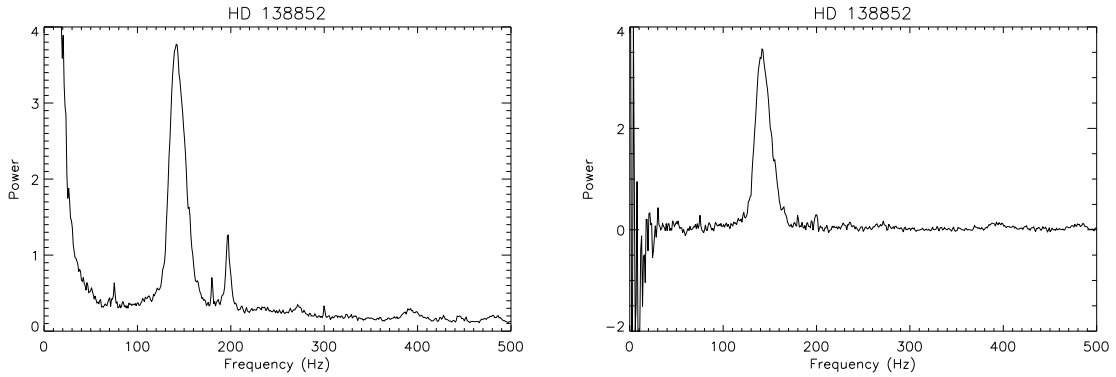

FIGURE 6. An example of a raw power spectrum (left) showing a combination of the fringe signal, photon noise, scintillation noise and camera noise. The peak due to the fringes look Gaussian instead of square due to atmospheric seeing. Once the noise has been measured and removed only the fringe signal remains (right).

simply be subtracted from the data power spectra before performing the integration. An example of this is given in Figure 6. I will describe how this is done in the following sections on implementation of this method for CLASSIC and CLIMB.

This calculation can be performed for each fringe scan and a mean and standard deviation found for V^2. In the data reduction pipeline this is referred to as the V2_SCANS estimate.

There is one more correction that can be made to the visibility estimate. Because of atmospheric turbulence, the visibility is changing constantly and so can be considered to be a random variable with some mean $\overline{V}$ and a variance σ_V^2. Since we are measuring the mean of the square of the visibility, we are actually measuring

$$\overline{V^2} = \overline{V}^2 + \sigma_V^2, \tag{48}$$

and thus all estimates of the square of the visibility are biased by the variance of the visibility. Unfortunately, it is not possible to take the square root of S as, due to the statistical nature of the measure, it is sometimes negative. It is, however, possible to square S, resulting in an estimate of $\overline{V^4}$. If one assumes the statistical distribution of the correlation is normal, one can then form the unbiased estimator for the correlation

$$\overline{V} = \left(\frac{3\overline{V^2}^2 - \overline{V^4}}{2} \right)^{\frac{1}{4}} \tag{49}$$

with the corresponding variance estimate

$$\sigma_V^2 = \sqrt{\overline{V}^4 - \frac{1}{2}(\overline{V^2}^2 - \overline{V^4})} - \overline{V}^2. \tag{50}$$

In the data reduction pipeline this is known as the V_NORM estimator.

Since the real visibility can never be negative, it is sometimes better to use a log-normal distribution, normally parametrized using the variables μ and σ^2. These can be determined using

$$\mu = \frac{1}{4} \ln \frac{\overline{V^2}^4}{\overline{V^4}} \tag{51}$$

and

$$\sigma^2 = \frac{1}{4} \ln \frac{\overline{V^4}}{\overline{V^2}^2} \tag{52}$$

from which we get the unbiased correlation estimate

$$\overline{V} = \exp(\mu + \frac{1}{2}\sigma^2) \tag{53}$$

with the variance

$$\sigma_V^2 = \exp(2\mu + 2\sigma^2) - \exp(2\mu + \sigma^2). \tag{54}$$

In the data reduction pipeline this is known as the V_LOGNORM estimator.

In practice the normal and log-normal equations give virtually the same results during times of good seeing, or high visibility, and typically diverge at very low signal to noise.

2.4.3. Implementation of the Amplitude Estimator for CLASSIC

There are several ways to form an expression similar to the simple fringe Equation 29. Since there are two outputs in the CLASSIC beam combiner, one can derive a visibility estimator for each output, as well as one for the difference between them. In this document we will focus on the difference signal, largely because it is relatively immune to common noise such as scintillation.

We begin by considering Equation 22, which shows that the two outputs of CLASSIC present fringes in anti-phase, but whose amplitude is changed in each case by the transfer functions defined in Equation 20. In an ideal world these transfer function would be the same, but any misalignment of the beam combiner optics can result in a difference. We must therefore calculate T_{1AB} and T_2AB separately. This is one reason why there are shutter sequences in the standard method of collecting the data. A shutter sequence in CLASSIC consists of a series of scans with one shutter close, followed by another series of scans with both shutters close, and finally a series with the first shutter open and the second shutter closed. Before 2013 we had one short shutter sequence at the beginning, used by the on-line code for real time visibility estimation, and a longer shutter sequence at the end used by the data reduction pipeline. Since then, the second sequence kept both shutters open and moved the delay line carts off-fringe in order to directly measure the noise power spectra. These shutter sequences also provide estimates for both T_{1AB} and T_2AB, as well as a measurement of the background counts B_i in each channel.

With these measurements of the backgrounds and transfer functions of each output of CLASSIC we can now form the un-normalized estimator for each output

$$F_i(t) = (N_i(\sigma_0, \Delta\sigma) - B_i)/T_{iAB}. \tag{55}$$

where B_i is the mean background signal in output i as measured during the shutter sequences. We can then form the difference between these two signals

$$F(t) = (F_1(t) - F_2(t))/2.0. \tag{56}$$

All that remains is for us to normalize this expression

$$\begin{aligned} f_{\rm norm}(t) &= 2.0 \times F(t)/(\overline{F_1(t)} + \overline{F_2(t)}) & (57)\\ &= V\ \mathrm{sinc}\left[\pi\Delta\sigma v t\right] \cos\left[2\pi\sigma_0 v t + \Phi\right] & (58) \end{aligned}$$

where $\overline{F_i(t)}$ is the average value across the scan of each output. The result of all this is that Equation 59 produces a function of the form of the simple fringe Equation 29 and the analysis can continue as described above.

It remains for us to estimate the power spectrum of the noise in this signal. There are three main elements of this noise: scintillation, photon noise, and camera noise. Since the scintillation noise is present in both the output signals a great deal is removed when we take the difference between the two signals. As mentioned above, due to optical miss-alignments and differences in camera gain between the two output pixels, there will still be a little scintillation noise present in the signal, and this noise must be measured and removed.

Unlike the scintillation noise, the photon and camera noise can, in theory, be calculated given a good knowledge of the camera characteristics. In practice, however, we have found that since we need to measure the scintillation, we might as well measure these directly from the data. Fortunately, we have the data collection sequences before and after the fringe data, and it is relatively easy to estimate the total noise from these.

2.4.4. Old Shutter Sequence

Before the 2013, we used a duel shutter sequence on CLASSIC data, that is, there were two shutter sequences, both the same, with one before the data collection and one after. Each sequence has some data with each input beam by itself and one of just the background noise on the camera. For each part of the shutter sequence, beam A, no beams and beam B, we do exactly the same analysis as described above for the fringe data. This results in the three power spectra

$$\begin{aligned} \mathrm{PS}(f_A(t)) &= \mathrm{PS}(\Im_A(t)) + \mathrm{PS}(P_A(t)) + \mathrm{PS}(C(t)) && (59)\\ \mathrm{PS}(f_B(t)) &= \mathrm{PS}(\Im_B(t)) + \mathrm{PS}(P_B(t)) + \mathrm{PS}(C(t)) && (60)\\ \mathrm{PS}(f_{\mathrm{Dark}}(t)) &= \mathrm{PS}(C(t)) && (61) \end{aligned}$$

where here $\Im_i(t)$ is the scintillation in the signal with just input beam i, $P_i(t)$ is the photon noise with just input beam i, and $C(t)$ is the camera noise. We expect the noise in the output signal to contain the scintillation and photon noise from both input beams, but to have the camera noise just once. We therefore write the noise power spectrum in the signal to be:

$$\mathrm{PS}(\aleph(t)) = \mathrm{PS}(f_A(t)) + \mathrm{PS}(f_B(t)) - \mathrm{PS}(f_{\mathrm{Dark}}(t)) \quad (62)$$

and this must be subtracted from the fringe signal power spectrum of Equation 59

$$\mathrm{PS}(f(t)) = \mathrm{PS}(f_{\mathrm{norm}}(t)) - \mathrm{PS}(\aleph(t)) \quad (63)$$

and we can now perform the analysis set out in section 2.4.2.

2.4.5. New Shutter Sequence

At the beginning of 2013 we changed to having only a single shutter sequence at the beginning of the collection sequence. This can be used to calculate the transfer functions, the background counts, and also to get an estimate of the noise power spectra as described in the previous section for use in the on-line software system.

Instead of repeating the shutter sequence at the end of the data collection, we now move the delay line several centimeters away from the fringe location and collect a series of scans in

exactly the same way as the on-fringe scans. This is then analyzed in exactly the same way as the on-fringe data and provides a much better estimate of the background noise power spectrum PS($\aleph(t)$) than one derived from the shutter sequences described above.

2.4.6. Implementation of the Amplitude Estimator for CLIMB

Implementing the amplitude estimator for CLIMB is very similar to CLASSIC, except now we have three input and output beams and three baselines to deal with. The procedure is a little different for each baseline and so I will set them out separately here.

For each of the three outputs we again first subtract the mean background signal as measured during the shutter sequence, where in the case of climb we must measure the signal with all three shutters closed and then with each of the three shutters A,B and C open in turn. So we have the un-normalized signals

$$F_{i,\mathrm{unnorm}}(t) = N_i(\sigma_0, \Delta\sigma) - B_i. \tag{64}$$

We then obtain the normalized signal by dividing by the mean

$$F_i(t) = F_{i,\mathrm{unnorm}}(t)/\overline{F_{i,\mathrm{unnrom}}(t)}. \tag{65}$$

Having done this for each of the three output beams 1,2 and 3 we are ready to form the normalized fringe signal for each baseline

$$\begin{aligned}
f_{AB,\mathrm{norm}}(t) &= \left(F_2(t)/T_{2AB} - F_3(t)/T_{3AB}\right)/2 \\
&= V_{AB}\ \mathrm{sinc}\left[\pi\Delta\sigma v_{AB}t\right]\cos\left[2\pi\sigma_0 v_{AB}t + \Phi_{AB}\right] + O_{BC/CA}(t) \qquad (66)\\
f_{BC,\mathrm{norm}}(t) &= \left(F_1(t)/T_{1BC} + (F_2(t) + F_3(t))/(T_{2BC} + T_{3AB})\right)/2 \\
&= V_{BC}\ \mathrm{sinc}\left[\pi\Delta\sigma v_{BC}t\right]\cos\left[2\pi\sigma_0 v_{BC}t + \Phi_{BC}\right] + O_{AB/CA}(t) \qquad (67)\\
f_{CA,\mathrm{norm}}(t) &= \left(F_2(t)/T_{2CA} - F_3(t)/T_{3CA}\right)/2 \\
&= V_{CA}\ \mathrm{sinc}\left[\pi\Delta\sigma v_{CA}t\right]\cos\left[2\pi\sigma_0 v_{CA}t + \Phi_{CA}\right] + O_{AB/BC}(t) \qquad (68)
\end{aligned}$$

where we have added terms of the form $O_{BC/CA}$ to show that in the $F_{AB}(t)$ and $f_{CA}(t)$ signals actually include all three sets of fringes, but at difference frequencies. If we restrict the integration limits when we calculate the total power S_{ij} for each baseline we can separate out the fringes of interest in each case, and since we know the central frequency of each fringe this is not too difficult unless the seeing causes the power in the difference fringe signals to overlap.

In the case of the signal $f_{BC}(t)$, if all goes well, only the BC fringes will be present, but in practice there is often a small amount of leakage from the other fringes signals due to optical misalignment and imperfections in the optical coatings. Still, given that we know the correct integration range for the visibility analysis this does not present a problem.

It remains to estimate the noise power in each signal, which we can do in a way similar to CLASSIC.

2.4.7. Old Shutter Sequence

As for CLASSIC, before 2013 we used a shutter sequence before and after the collection of on-fringe data. The first shutter sequence can provide an estimate of the noise power

spectra for use by the on-line control system, while the second one is used in the data reduction pipeline.

We normalized signals for the shutter sequences in the same way we do for the fringe signals and then calculate the power spectra for each output beam. We then have the power spectra in each output beam for the background signal and for each input beam. So for each beam we have

$$\begin{aligned}
\mathrm{PS}(f_{iA}(t)) &= \mathrm{PS}(\Im_{iA}(t)) + \mathrm{PS}(P_{iA}(t)) + \mathrm{PS}(C_i(t)) && (69)\\
\mathrm{PS}(f_{iB}(t)) &= \mathrm{PS}(\Im_{iB}(t)) + \mathrm{PS}(P_{iB}(t)) + \mathrm{PS}(C_i(t)) && (70)\\
\mathrm{PS}(f_{iC}(t)) &= \mathrm{PS}(\Im_{iC}(t)) + \mathrm{PS}(P_{iC}(t)) + \mathrm{PS}(C_i(t)) && (71)\\
\mathrm{PS}(f_{i\ \mathrm{Dark}}(t)) &= \mathrm{PS}(C_i(t)) && (72)
\end{aligned}$$

where once again $\Im_{ij}(t)$ and $P_{ij}(t)$ are the scintillation and photon noise in output beam i due to input beam j, and $C_i(t)$ is the camera and background noise in output beam i.

From these we can now form the noise power spectrum present in each output pixel

$$\begin{aligned}
\mathrm{PS}(\aleph_1(t)) &= \mathrm{PS}(f_{1B}(t)) + \mathrm{PS}(f_{1C}(t)) - \mathrm{PS}(f_{1\ \mathrm{Dark}}(t)) && (73)\\
\mathrm{PS}(\aleph_2(t)) &= \mathrm{PS}(f_{2A}(t)) + \mathrm{PS}(f_{2B}(t)) + \mathrm{PS}(f_{2C}(t)) - 2\times\mathrm{PS}(f_{2\ \mathrm{Dark}}(t)) && (74)\\
\mathrm{PS}(\aleph_3(t)) &= \mathrm{PS}(f_{3A}(t)) + \mathrm{PS}(f_{3B}(t)) + \mathrm{PS}(f_{3C}(t)) - 2\times\mathrm{PS}(f_{3\ \mathrm{Dark}}(t)) && (75)
\end{aligned}$$

where we note that since in each of the output pixels 2 and 3 there are three input beams, and so we need to remove twice the background noise in order to correctly estimate the noise power spectra in these outputs.

It is now possible to calculate the noise power in the fringe power spectra of Equations 66, 67, and 68:

$$\begin{aligned}
\mathrm{PS}(\aleph_{AB}(t)) &= \left(\mathrm{PS}(\aleph_2(t))/T_{2AB}^2 + \mathrm{PS}(\aleph_3(t))/T_{3AB}^2\right)/4 && (76)\\
\mathrm{PS}(\aleph_{BC}(t)) &= \left(\mathrm{PS}(\aleph_1(t))/T_{2BC}^2 + (\mathrm{PS}(\aleph_2(t)) + \mathrm{PS}(\aleph_3(t)))/(T_{2BC}^2 + T_{3BC}^2)\right)/4 && (77)\\
\mathrm{PS}(\aleph_{CA}(t)) &= \left(\mathrm{PS}(\aleph_2(t))/T_{2CA}^2 + \mathrm{PS}(\aleph_3(t))/T_{3CA}^2\right)/4. && (78)
\end{aligned}$$

These must be subtracted from the fringe signals to obtain the noise free signals

$$\begin{aligned}
\mathrm{PS}(f_{AB}(t)) &= \mathrm{PS}(f_{AB,\mathrm{norm}}(t)) - \mathrm{PS}(\aleph_{AB}(t)) && (79)\\
\mathrm{PS}(f_{BC}(t)) &= \mathrm{PS}(f_{BC,\mathrm{norm}}(t)) - \mathrm{PS}(\aleph_{BC}(t)) && (80)\\
\mathrm{PS}(f_{CA}(t)) &= \mathrm{PS}(f_{CA,\mathrm{norm}}(t)) - \mathrm{PS}(\aleph_{CA}(t)) && (81)
\end{aligned}$$

suitable for the analysis set out in section 2.4.2.

2.4.8. New Shutter Sequence

Since the beginning of 2013, the second shutter sequence has been replace with a sequence of off-fringe data by moving the delay lines away from the fringe position and collecting

the same number of scans as the on-fringe fringe data. These can then be analyzed in an identical manor to the on-fringe data providing an excellent estimate of the noise power spectrum. As for CLASSIC, the shorter shutter sequence at the beginning is use to estimate the background counts and the transfer functions, as well as an estimate of the noise power spectra for use by the on-line control system.

2.5. Extracting Closure Phase from the Data

One important, and perhaps most difficult, part of measuring closure phase is ensuring that the signs on all the various parts, and on the final closure phase itself, are all correct. Of primary importance in getting this right is making sure you are forming closed triangles of phases, and not open triangles. For example, in an instrument that creates fringes in the image plane, for example an aperture mask instrument, you need to use the phase of the negative frequency of the the highest frequency component of the phase, that is, the frequencies need to add to zero in order to obtain true closure. In other words, you must form the complex triple amplitude of the two lowest frequencies and the conjugate of the highest frequency. In the case of CLIMB, we must also be very careful about the signs of the various phases.

First, or course, we must obtain a measurement of the phase of the fringes on the three baselines represented in the instrument. Referring back to Equations 25, 28, and figure 4, we recall that the fringes in each baseline are formed at three different frequencies of $f_{CA} = 1/v$, $f_{BC} = 2f_{CA}$ and $f_{AB} = 3f_{CA}$, where we are for now ignoring the sign on these frequencies. Thus the fringes occur at multiples of the lowest frequency fringe. since we know the sample rate of the detector and the fringe frequencies, it is relatively easy to extract a segment of that contains only one cycle of the lowest frequency fringe. Thus if we are sampling at a frequency of $f_{\rm samp}$ Hz, we will use a segment that is $f_{CA}/f_{\rm samp}$ samples in length. In almost all cases we arrange things so that this is a integer multiple of 3. The default at the time of writing this document is to have 5 samples across the highest frequency fringe, and so one segment would be 15 samples in length. It is also common to use less than this default, where the minimum useful rate is 3 samples per fringe, or 9 samples per segment. An example segment of real, albeit very high signal to noise, data is given in the upper plot of Figure 7.

The Fourier Transform of this segment will contain, in the first four bins, the DC, one cycle, two cycle, and three cycle per segment complex amplitudes, that is the DC component and the three frequencies of the three fringes we are interested in. The lower plot of Figure 7 shows the power spectrum of the example segment. Note how almost all the power is contained in the first three frequency bins. We can therefore extract quite easily the amplitude and phase of the three fringe patterns $F(f_{AC})$, $F(f_{CB})$, and $F(f_{AB})$. Note that it is at this point that we need to be careful about the sign of the phases. The CA fringes are reversed due to the geometry of the beam combiner, while the BC are reversed due to the motion of the dither mirrors. We therefore use the triple product

$$A_{ABC} = F(f_{AB}) \times F^*(f_{BC}) \times F^*(f_{AC}) \tag{82}$$

as our estimator for the closure phase. One final wrinkle is to take into account that the dither mirrors move both forward and backwards on alternate scans and so, given our definition of Phi_{ij} being positive when the phase of i is ahead of the phase of j, we need to take the conjugate of the entire triple product A^*_{ABC} on each alternate scan. In this way, it is possible to obtain a triple product, both amplitude and phase, for each segment in each fringe scan, as shown in Figure 8.

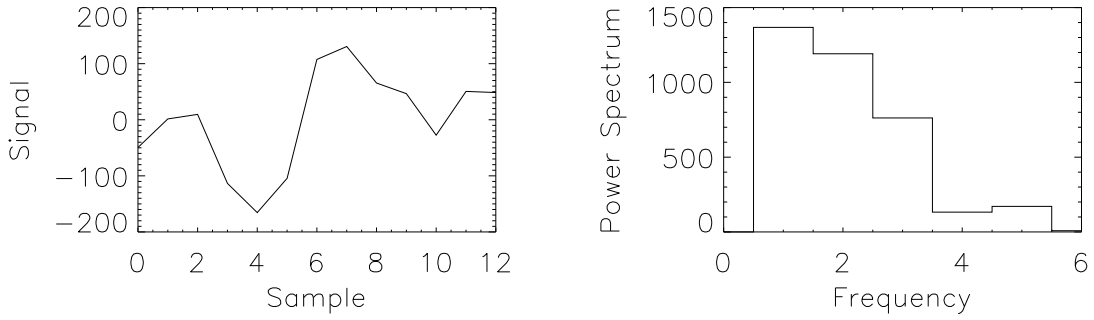

FIGURE 7. Example of extracting the closure phase signal from a single segment. The plot on the left shows the raw signal in output pixel B of a single high SNR segment. The plot on the right shows the power spectrum of this segment. Note that almost all the power is in the first three non-zero frequency bins representing the fringe with one cycle per segment (CA), two cycles per segment (BC) and three cycles per segment (AB).

This calculation can be performed on each scan in the data set. The final closure phase estimate is produced by first taking the mean of the triple product across all scans, and then calculating its phase. This means we have a closure phase estimate weighted by fringe amplitude. Of course, there is little point in keeping track of those segments in which we know no fringes exist, so the actual data reduction code looks for fringe overlap and other things, such as whether fringes appear in the scan at all. These issue will be discussed in the following sections.

A last, but very important, consideration is the final sign of the closure phase estimate. All of the calculations described above have been performed with respect to the input beams of the beam combiner, and what we are really interested is on the UV coordinates of the telescopes these represent on the sky. This calculation is not difficult given the position of the star on the sky and the, assumed well known, positions of the telescopes on the ground (see for example Equation 12.1 in Dyck (1999) or Equation 4.3 in Thompson et. al. (2001)). However, try as I might I have failed to find an overt definition of the sign convention of closure around a triangle of telescopes[7] but it appears most common to say that when looking from above the sign of the closure is positive going anti-clockwise around the triangle of telescopes, and this is the convention used in the CLIMB data reduction pipeline. In the end what really matters is that you use the same convention in both you reduction and imaging/modeling software.

3. REFERENCES

Benson et. al., "Technique for obtaining visibility amplitudes from atmospherically disturbed interferograms", Ap.O., **34**, 51, 1995

Born and Wolf, "Principles of Optics", Perganmon Press, New York, WHAT YEAR IS THIS????

T.A. ten Brummelaar, "Differential path considerations in optical stellar interferometry", Ap. Opt., **34**, 2214, 1995

[7]If anyone reading this knows of one I'd appreciate hearing about it

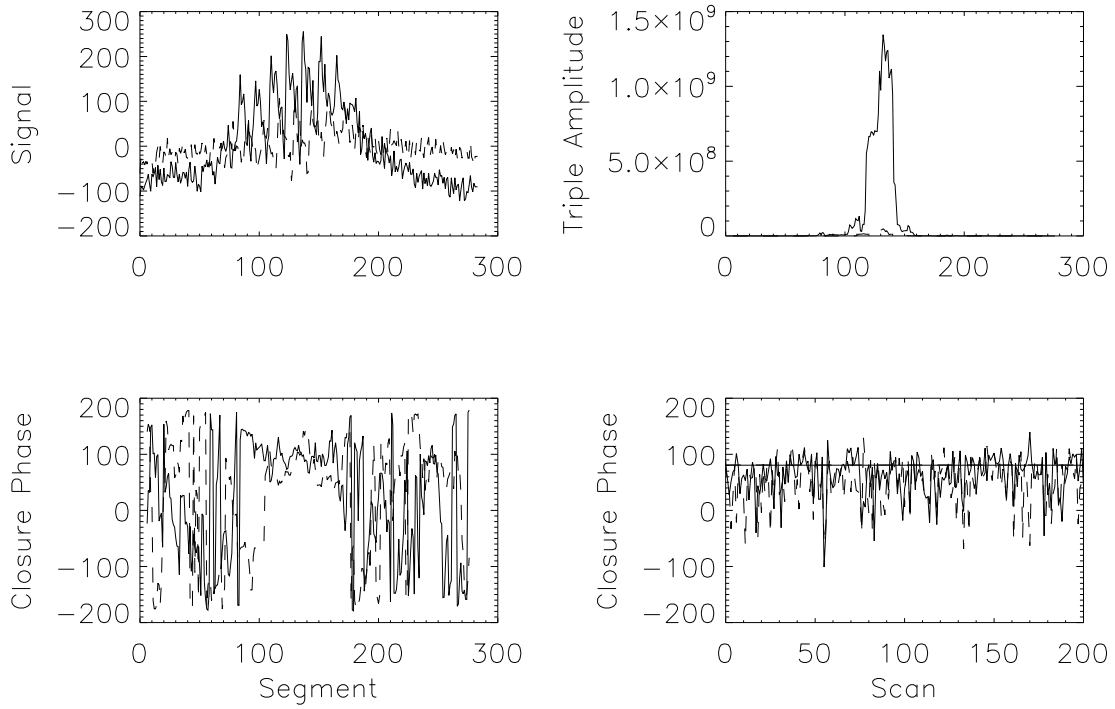

FIGURE 8. Example of extracting the closure phase signal from a single scan. The top left plot shows the raw signals in output pixels B (solid line) and C (dashed line) of a single high SNR scan. The top right plot down shows the triple product amplitude of the signals. The bottom left plot down shows the closure phase of the two signals, or phase of the triple product. Note how the closure phase is random in the places where the triple product amplitude is zero. The plot at the bottom right shows the triple product amplitude weighted means of the closure phase signals of all scans in the data file.

T.A. ten Brummelaar et. al., "First Results from the CHARA Array. II. A Description of the Instrument", Ap.J., **628**, 453, 2005

D. O'Brien et al., "Inner Orbits in Hierarchical Triple Systems from the CHARA Array IL V819 Her B", Ap.J., **728**, 111 2011

P.H. van Cittert, Physica, **1**, 201, 1934

H.M. Dyck "Interferometry with Two Telescopes", in Principles of Long Baseline Interferometry, Ed P.R. Lawson, NASA/JPL, 1999

W.H. Press et al., "Numerical Recipes in C", Cambridge Uni. Press, 1992

A.R. Thompson, et al., "Interferometry and Synthesis in Radio Astronomy", John Wiley & Sons, New York 2001.

F. Zernike, Physica, **5**, 785, 1938

Zetie et. al., "How does a Mach-Zehnder interferometer work?", Phys. Educ, **35**, 46, 2000